

# Hydrogeological interferences in tunneling - A comprehensive study

Roberto Marzocchi, Sebastian Pera & Hans-Rudolf Pfeifer

**Abstract:** The interference of groundwater with tunneling is both an environmental and an engineering problem. In fractured rocks, the prediction of tunnel water inflows is of primary importance, but unfortunately it is very complex, even impossible without the development of a well-founded Conceptual Hydrogeological Model (CHM). For this purpose, a comprehensive study is ongoing in the region of Monte Ceneri close to Lugano (Ticino, Switzerland), where a tunnel of 16 km in length is under construction in metamorphic rocks (gneiss and amphibolites). In particular, we are integrating the structural geological informations, commonly used for tunnel design, with geophysical surveys (VLF electromagnetic and resistivity) and physico-chemical data (discharge, temperature, electric conductivity, pH, ionic and stable isotope composition) of water collected at the surface and within the tunnel actually in construction. The theoretical frameworks and the preliminary results of the research are presented.

**Keywords:** Groundwater, Tunneling, Conceptual model, Geochemical method, Geophysical survey, Southern Switzerland

**Roberto MARZOCCHI** ✉

**Sebastian PERA**

Istituto Scienze della Terra (IST-SUPSI)  
Via Trevano C.P. 72  
CH-6952 Canobbio - Switzerland  
FAX: +41 (0)586666209

**Hans-Rudolf PFEIFER**

IMG - Centre d'Analyse Minérale,  
Faculté des Géosciences et de l'Environnement  
Université de Lausanne, Anthropole  
CH-1015 Lausanne - Switzerland  
Hans-Rudolf.Pfeifer@unil.ch

**Roberto MARZOCCHI** ✉

roberto.marzocchi@suspi.ch

**Sebastian PERA**

sebastian.pera@suspi.ch

**Riassunto:** Le acque sotterranee costituiscono circa il 98% delle risorse acquifere allo stato liquido nel mondo, e la loro conservazione è una questione di primario interesse.

In particolare nel Canton Ticino (Svizzera) le acque sotterranee sono la principale risorsa di acqua potabile: circa il 90% di esse deriva infatti dagli acquiferi vallivi o dalle sorgenti. La necessità di nuove vie di comunicazione europee (strade e ferrovie) ha determinato l'esigenza di costruire nuove gallerie in difficili condizioni geologiche. In particolare il Nord Italia e la Svizzera sono regioni strategiche per i trasporti Europei; esse sono infatti una via obbligata tra il Mar Mediterraneo e l'Europa del Centro Nord.

Nelle regioni alpine infatti, molte infrastrutture sia in superficie che sotterranee sono state costruite anni fa (ad es. la ferrovia e l'autostrada del Gottardo), mentre molte altre sono ad oggi in costruzione, come la nuova ferrovia ad alta velocità del Gottardo, che permetterà un collegamento più veloce tra Zurigo e Milano ed è certamente una delle più importanti attualmente in costruzione. Nell'ambito di questa nuova infrastruttura, denominata Alptransit, in particolare, le gallerie del S. Gottardo e del Monte Ceneri, rispettivamente lunghe circa 57 e 16 km, sono attualmente in fase di costruzione.

Per queste ragioni, attualmente c'è un'esigenza crescente di coordinare tutti gli aspetti idrogeologici durante la costruzione della nuova galleria al fine di migliorare la sostenibilità ambientale. Inoltre lo scavo di questa galleria è un'opportunità unica per acquisire una buona conoscenza geologica e idrogeologica del sito. Specialmente per le regioni montuose la corretta previsione del flusso delle acque nella matrice rocciosa non è infatti semplice, in quanto la permeabilità primaria delle rocce cristalline è praticamente nulla e solo la presenza di fratture, faglie e altre cavità permette il flusso delle acque. Pertanto la corretta valutazione dei parametri acquiferi delle rocce fratturate è difficile o impossibile senza studi idrogeologici di dettaglio.

Per questo scopo, intendiamo utilizzare indagini geochimiche, tra cui le metodologie isotopiche, e geofisiche per comprendere meglio il deflusso idraulico sotterraneo in roccia fratturata e ottenere un affidabile modello idrogeologico concettuale.

Abbiamo quindi intrapreso un'indagine di ricerca nel Canton Ticino, in particolare nella zona vicina a Lugano, dove si sta attualmente scavando la galleria di base del Monte Ceneri.

Quest'area è principalmente costituita da rocce metamorfiche (gneiss e anfiboliti), generalmente considerate impermeabili, tuttavia le fratture e i processi legati agli agenti atmosferici localmente aumentano la permeabilità, permettendo il flusso delle acque.

In questo articolo intendiamo descrivere per prima cosa gli assetti geologici ed idrogeologici dell'area di studio, per poi illustrare l'approccio geochimico e geofisico concepito ed i risultati preliminari delle prime applicazioni.

Received: 25 may 2010 / Accepted: 29 november 2010  
Published online: 31 december 2010

© Scribo 2010

## Geological and hydrogeological settings of the area

The Ceneri base tunnel is entirely located within the crystalline basement of southern Alps. From a tectonic point of view, this geological zone is separated from the Penninic nappes of the Central Alps by the *Insubric Line* (known also as *Periadriatic Line*), which is one of the main tectonic features of the Alpine chain.

The Southalpine basement extends along the whole length of the tunnel from the Vigana north portal (Magadino alluvial plain), to the Vezia south portal (Vedeggio alluvial plain).

The part of tunnel drilling is mainly constituted by metamorphic rocks (gneisses and amphibolites). However it is possible to subdivide the area where tunnel will be drilled in two different zones (Pini et al. 2007), that are separated by a fault, the *Val Colla Line* (the black broken line that intersect the tunnel in figure 4):

- the Ceneri zone, in the north, 10.2 km long;
- the Val Colla zone, in the south, 4.6 km long.

In particular, the first zone is essentially constituted by ortho- and paragneisses, Ceneri orthogneisses and other heterogeneous gneisses of Giumello-type, greenschists, amphibolites and serpentinites, i.e. basic and ultrabasic rocks present in a small area under Gola di Lago. The zone of Val Colla is essentially constituted by the following main lithologies: metasedimentary rocks, S. Bernardo orthogneisses, Stabiello paragneisses and schists.

The main schistosity is nearly parallel to the slope in the northern area, while in the southern part it is south or south/east dipping. The deformations associated to the alpine orogenesis are of destructive nature with several clastic structures, such as fault zones and fractures, which in the overlying landscape, morphologically correspond to incisions in the slope.

The topographic elevation of the gneiss bodies of the Ceneri zone ranges from 300 and 1100 m a.s.l., while in the Val Colla zone it ranges

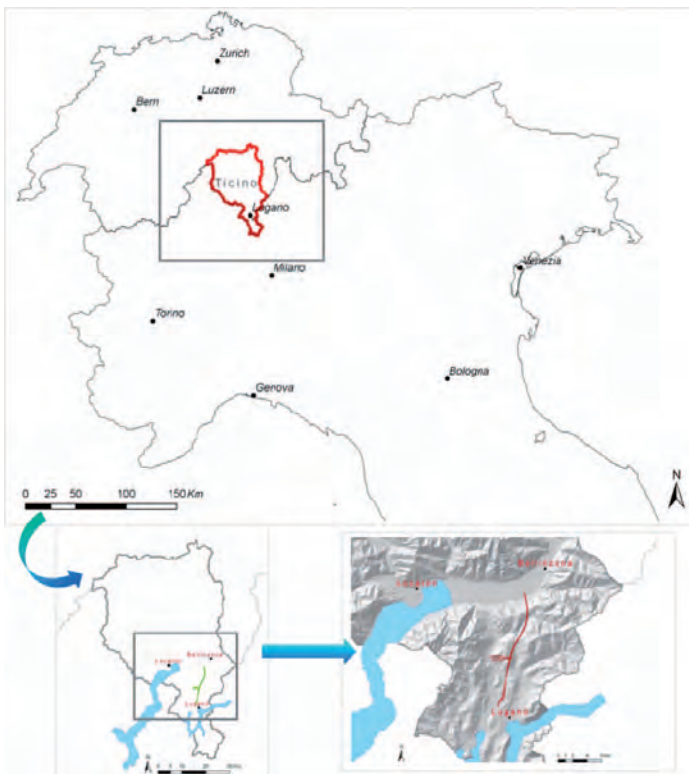


Fig. 1: Area of Ticino Canton where the Monte Ceneri base tunnel is drilled

es from 300 and 500 m a.s.l. The Ceneri base tunnel passes through the gneiss bodies at an elevation of about 250 m a.s.l.

In figure 5 all expected lithologies of the tunnel are shown, while figure 4 illustrates a horizontal cut through the tunnel and a geological sketch map (scale 1:250000), which also contains the most important known disturbed zones.

All the crystalline rocks crossed by tunnel, are usually considered impervious (low absolute permeability), however fractures and other alteration processes locally increase the effective permeability, allowing water flow in the rock matrix. It is not simple to assign values to the permeability index  $k$ . In fact it depends substantially of the fracture abundance and of their interconnection. Several studies have investigated the permeability range of the crystalline rocks.

In particular Beatrizzotti (1996) has studied the permeability of the rock in the Ticino Canton. With a series of pumping tests, he measured a value of  $k = 1.7 \cdot 10^{-6}$  m/s in the Ceneri gneiss, and  $k = 1 \cdot 10^{-6} \div 4 \cdot 10^{-6}$  m/s in the Stabiello gneiss in the zone of Val Colla. (all these data refer to surface rocks).

Several literature studies have shown a depth-dependency of the hydraulic conductivity in crystalline rocks such as gneisses, not confirmed instead in other crystalline rocks such as granites and basalts. In particular, in gneiss, a hydraulic discontinuity has generally been observed under the uppermost 100-200 m. In fact, close to the surface substantially higher conductivities are registered, due to higher fracture density and higher apertures; while stress release, weathering processes and gravitationally induced weakening of the bedrock along steep slopes cause a decrease of the permeability with depth. Therefore in gneiss it is so possible distinguish an uppermost zone (Oftringer, 2001; Maréchal and Etcheverry, 2003), often named “decompressed”, and, deep down, an other zone that is named “deeper” and is characterized by a lower permeability (Fig.2).

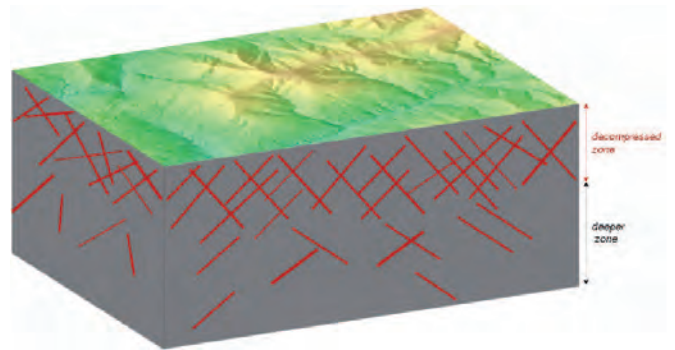


Fig. 2: Simplified pattern of the hypothetical presence of fractures in gneissic rocks.

This evidence is described by a number of literature studies performed in the crystalline rocks of the Alps. In particular, Maréchal and Etcheverry (2003), on the basis of the data collected in the M. Blanc massif and in other Alpine crystalline basements, propose an exponential decrease of hydraulic conductivity described by equation 1, that is commonly adopted for the design of structures in the deep rocks, such as tunnels or underground nuclear waste disposals.

$$k = k_0 \cdot e^{-\alpha \cdot C} \quad (1)$$

Where  $k_0$  (m/s) represents the hydraulic conductivity at the surface,  $C$  is the overburden (m) and  $\alpha$  is a parameter that Marechal and Etcheverry define as shown in table 1.

**Tab. 1:** Values of the  $\alpha$  parameter of equation 1.

| Zone   | $\alpha$ (m <sup>-1</sup> ) |
|--|-----------------------------|
| Uppermost decompressed zone (0-100 m)        | 0.05                        |
| Intermediate decompressed zone (100 - 600 m) | 0.015                       |
| Deeper zone (>600 m)                         | 0.005                       |

Therefore, the values of  $k$  at the tunnel depth, estimated on the basis of geological knowledge, drilling, Lugeon tests, pumping tests and variable head tests performed by tunnel designer, are in the range of  $1.8 \cdot 10^{-7} \div 7.5 \cdot 10^{-10}$  m/s. They are defined for different homogeneous intervals, that are the tunnel shares with similar geological features.

The total drainage due to tunnel excavation has been estimated within the geological design using the following the Muskat or Goodman formulation of formula 2 (El Tani, 2003) applied to homogeneous intervals.

$$Q = 2\pi \cdot k \frac{h}{\ln(2h/r_e)} \quad (2)$$

where  $r_e$  is the equivalent radius (8 m as estimated by designers) and  $h$  is the overburden above the tunnel. The drainage water is so evaluated using the value of  $k$  above discussed, and the most probable total discharge forecasted for both the base tunnel and the Sigrino exploration tunnel is 49 l/s (about 16 l/min/100m), while the conservative evaluation is 84 l/s (about 28 l/min/100m). In figure 3 the measured water inflows in the geological investigation tunnel of Sigrino, registered in the excavation phases, which is now monthly recorded are shown. Due to the high tunnel overburden and the good state of rocks, the inflows in the Sigrino tunnels are indeed very low.

From a qualitative point of view, the permeability of rocks crossed by the Ceneri base tunnel is generally low.

On the basis of the geological inspections (geomorphological and surface geological surveys, drilling inspections, previous geological informations, etc.) the tunnel excavation will be conducted in essentially dry conditions.

One of the most important disturbed zone, the Val Colla Line (Fig. 4 e 5), from drilling inspections seem be mainly composed by mylonites, that are fine grained shists, often with an high mica content and therefore essentially low permeable. A possible disturbed zone more permeable is localized under the Isona town (Fig 5), and finally the most important water inflows are expected close to the north and south portals, where the tunnel will be excavated in the decompressed zone.

## Geochemical methods

Geochemical methods consisted in monitoring springs and, if possible, water inflows in tunnel, for discharge, electric conductivity, pH and in collecting water samples for geochemical and isotopic analysis.

Both conductivity values, that are mostly related with Total Dissolved Solids (TDS), or the sum of major ions, allow defining different hydrogeological facies and can be an useful indicator of interactions between water and rocks, and thus of the water flows in the fractured rocks. Also discharge and temperature variability during the year, their comparison with rain events and mean monthly air temperature data can give further informations about spring types (e.g. deep or shallow groundwater systems).

The knowledge of the stable isotopic composition of atmospheric precipitations is an important research tool in the fields of hydrology, as well as of climatology and paleoclimatology. In fact, the water may be divided into light (<sup>1</sup>H<sub>2</sub><sup>16</sup>O) and heavy (<sup>1</sup>H<sub>2</sub><sup>16</sup>O and <sup>1</sup>H<sub>2</sub><sup>18</sup>O) molecules and the isotopic fractionation that occurs during chemical reactions and physical hydrological processes is a tool to understand the water provenance (Sheppard, 1986). For geochemical purposes, the isotopic compositions are expressed in terms of deviations relative to a standard material. Consequently,  $\delta$ -values are used to express

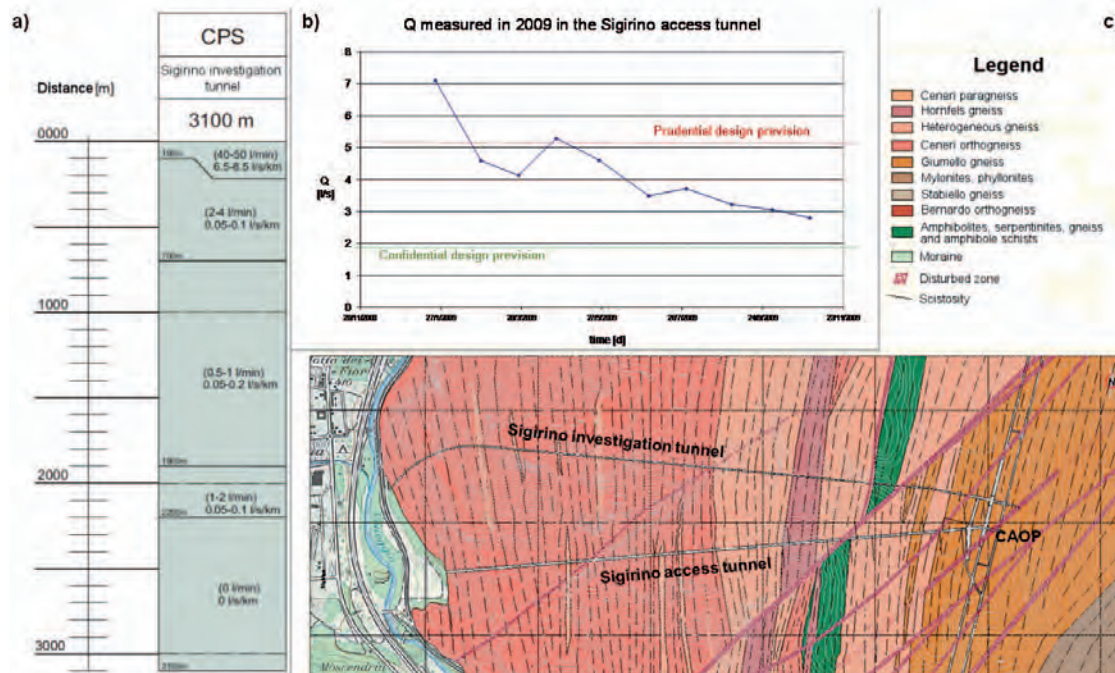


**Fig. 3:** Water inflows registered in the geological investigation tunnel during drilling phases(a) and actually (b) and corresponding lithologies crossed (c) (data kindly offers by Altransit Inc).



For example, *seasonal effect* (Fig. 6) can be useful in order to understand aquifer recharge, transit time of water in the rock, attenuation and flow rates (Eichinger et al., 1984; Maloszewski et al., 1990). For instance, in our study we will compare the seasonal variations of isotopic signature of the rain of Canton Ticino and the isotopic signature of monitored springs. From this type of data, that we are now collecting in the region surrounding the Monte Ceneri, we expect interesting information about water provenance and transit time. Investigating the *Altitude effect* is another interesting and widely used application in isotope hydrology. It consists of the identification of the elevation at which groundwater recharge takes place. In fact, as a rule, the isotopic composition of precipitations changes with the altitude of the terrain and it becomes more and more depleted in  $^{18}\text{O}$  and  $^2\text{H}$  at higher elevations. The observed effect on the  $^{18}\text{O}$  abundance generally varies between  $-0.1\text{‰}$  and  $-0.6\text{‰}$  per 100 m of altitude. Values in this range have also been reported for other mountainous regions in Switzerland (Pearson et al., 1991). However, the altitude effect is variable from region to region and unfortunately Pearson et al. in their technical report (Fig. 7) did not report any specific relationship that correlate elevation and isotopic abundance in Southern Switzerland. From a literature review, we found three possible relationships  $H\text{-}\delta^{18}\text{O}$  obtained for areas close to the Ticino canton (Fig. 8). The first is obtained by Ofterdinger et al (2001) and it is applied for the Gotthard region; it is certainly valid for the central Swiss Alps for data of that area, but probably not suitable for ours:

$$\delta^{18}\text{O} = - (0.0023 \pm 0.0003)z - (9.4 \pm 0.5)\text{‰} \quad (4)$$

A second relationship has been described by Pastorelli et al. (1999) for the Blenio Valley, but unfortunately on the basis of too few samples and it is most likely not valid for our area:

$$\delta^{18}\text{O} = - 0.00192 \cdot z - 7.51 \text{‰} \quad (5)$$

A third is obtained by Bestenheider (2006) also applied for the Blenio Valley on the basis of data collected until 2003 in the stations of Locarno-Monti, Riazino (Ticino river) and Grimsel.

$$\delta^{18}\text{O} = - 0.0024 \cdot z - 6.97 \text{‰} \quad (6)$$

Probably, not any of these relationships is reliable for our region. This lack may be a problem; in fact, in the alpine regions, it is necessary to take into account at least two different altitude gradients,

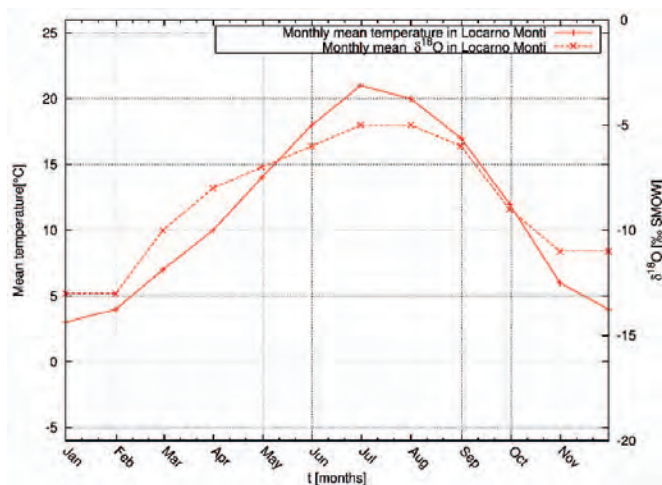


Fig. 6: Monthly mean isotopic composition of rain and temperature in Locarno

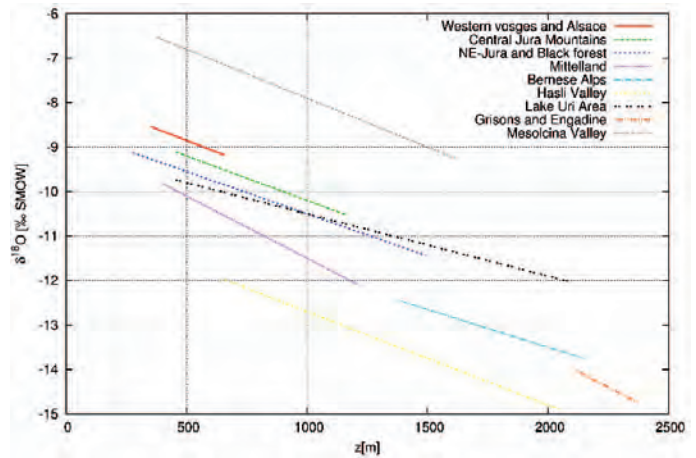


Fig. 7: Stable isotope-recharge altitude relationship for Northern Switzerland (elaborated from data reported in Pearson et al., 1991)

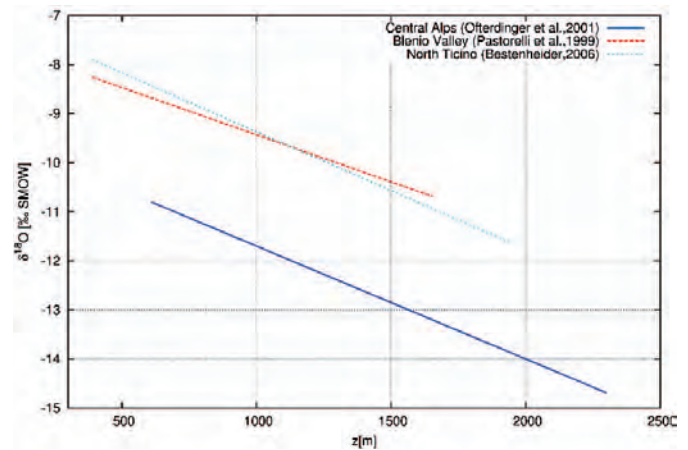


Fig. 8: Stable isotope-recharge altitude relationships obtained with data of area close to the Canton Ticino.

The difference in altitude gradients, between two regions at similar latitude and orography, but with a rain system that differs a lot, is considerable (fig.9). Therefore, it is clear that to obtain a good indication about mean altitude recharge, we need to find a valid relationship between altitude and isotopic composition of our rain.

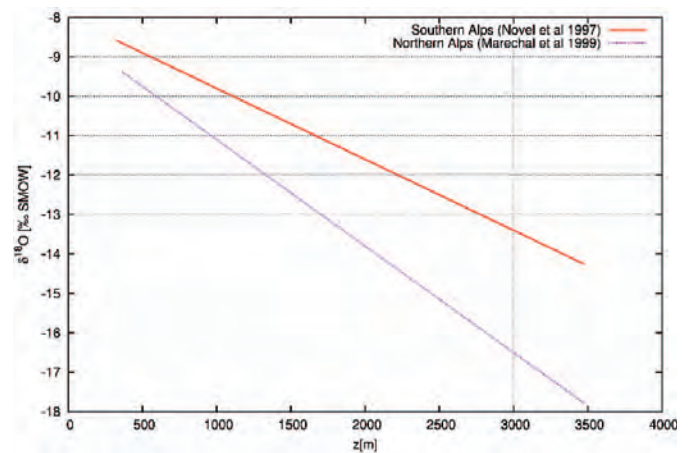


Fig. 9: Stable isotope-recharge altitude relationships for northern and southern Alps

because of the climatic contrast between the northern and southern sides of the mountains (Marechal and Etcheverry, 2003). For instance for the Southern Alps, Novel et al. (1999) have calculated an altitude gradient on 8 stations of precipitations lying between 315 and 3500 m in the Aosta Valley (Italy) during the 1993-1994 period. The relationship between the average annual content of  $^{18}\text{O}$  of precipitation and altitude is thus:

$$\delta^{18}\text{O} = - (0.0018 \pm 0.0002)z - (8 \pm 0.5)\text{‰} \quad (7)$$

While for the Northern Alps it seems possible to use the following relationship obtained by samples collected between the stations at Thonon les Bains (385 m) and Grimsel (1980 m):

$$\delta^{18}\text{O} = - 0.0027 \cdot z - 8.4 \text{‰} \quad (8)$$

The difference in altitude gradients, between two regions at similar latitude and orography, but with a rain system that differs a lot, is considerable (Fig. 9). Therefore, it is clear that to obtain a good indication about mean altitude recharge, we need to find a valid relationship between altitude and isotopic composition of our rain.

For this reason, we have densified the monitoring network of rain isotopic data for the Ceneri zone. In a first step we will measure data even in the Arosio rain gauge (Fig.10), that is located at 860 m a.s.l. and is close to the M. Ceneri base tunnel area. The data collected, that will be correlated with that collected in Locarno Monti (379 m a.s.l.) and eventually with others data, coming from GNIP stations, will hopefully allow us to obtain a reliable value for altitude gradient curve for the Monte Ceneri base tunnel area. Unfortunately, there is not yet a good collection neither of data for Northern Italy, where the only precipitation data actually available was sporadically collected in the 2002-2004 years and are reported in Longinelli et al. (2006).

Due to the lack of neighborhood data, recently we have increased the precipitation monitoring network with more five stations located

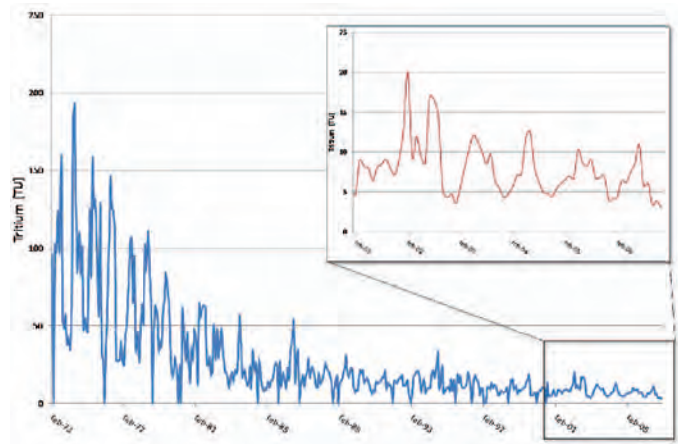


Fig. 11: Monthly values of tritium concentrations since 1972 in Locarno precipitations.

at different altitude in the Ticino Canton to get a better data set for the Southern Switzerland. Concerning data are not yet available, to this reason the stations will be present in further specific reports.

The tritium ( $^3\text{H}$ ) is a further isotopic element useful to obtain information about groundwater age, flow paths and velocities. It is first of all a radioactive heavy isotope of hydrogen, that is naturally formed in the upper atmosphere from a nuclear reaction between atmospheric nitrogen and thermal neutrons. The  $^3\text{H}$  thus formed enters the hydrologic cycle after an oxidation that forms "tritiated waters"  $^1\text{H}^3\text{HO}$ , and it finally decays to form helium  $^3\text{He}$ , that is named tritiogenic helium. The rate of radioactive decay is by convention expressed as the half-life  $T_{1/2}$ , defined as the time span during which a given concentration of the radioelement atoms decay to half the initial value. The half-life of tritium was calculated by Lucas and Unterweger (2000) as 12.32 years. Under undisturbed natural conditions the  $^3\text{H}$  concentration in

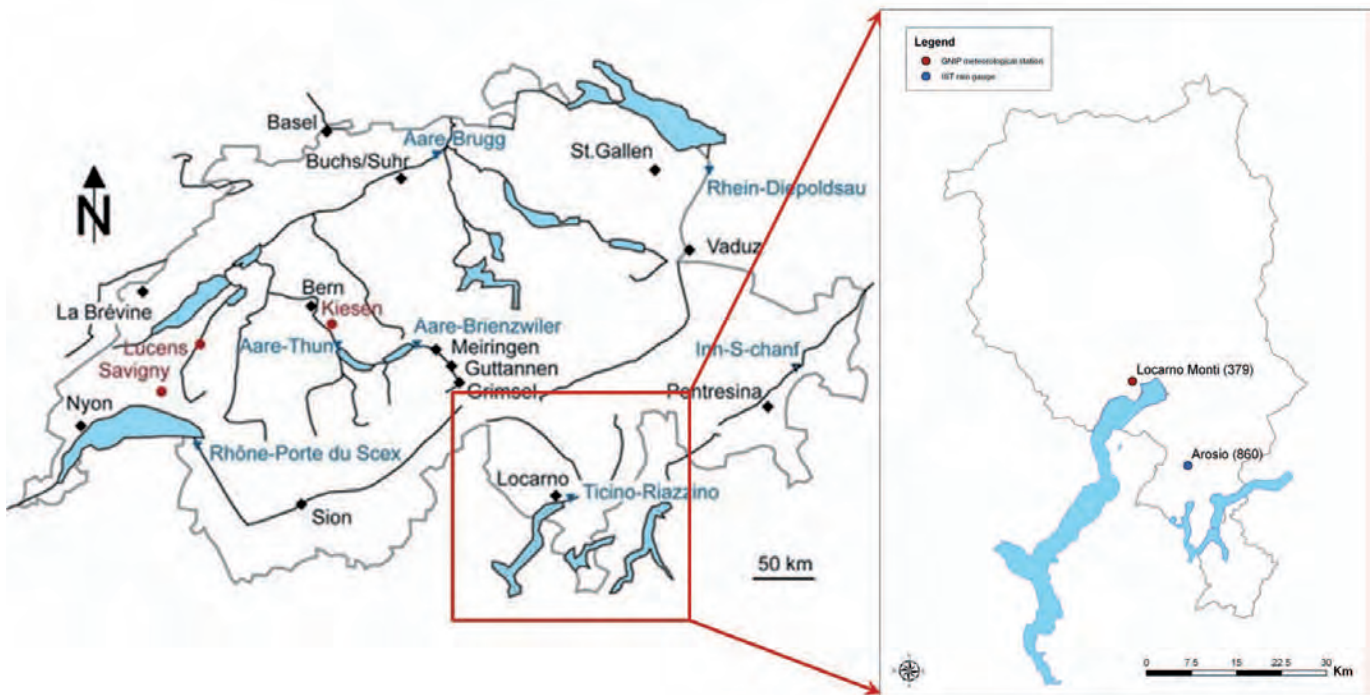


Fig. 10: Localization of precipitation isotope measurement stations of GNIP network and of Isonne rain gauge of Institute of Earth Sciences (SUPSI), used for this research project.

precipitations would be probably about 5 TU; however following the nuclear weapon tests of the early sixties, the  $^3\text{H}$  content in precipitation temporarily increased by a 1000-fold in the northern hemisphere. Since 1963, due to the end of the era of thermonuclear bomb testing in the atmosphere, this extreme  $^3\text{H}$  content has decreased to essentially natural values in winter when a large part of  $^3\text{H}$  stay in the stratosphere, while it increases about twice natural values in summer, when this part of  $^3\text{H}$  returns to the troposphere (Fig.11).

Actually the use of only tritium data is probably not able to give us detailed information on groundwater, especially in case of modern water, allowing only a qualitative interpretation of groundwater mean residence times. Rather the use of the tritium/helium-3 ( $^3\text{H}/^3\text{He}$ ) method (Schlosser et al., 1988; 1989; Aeschbach-Hertig et al., 1998; Althaus et al, 2009; Holzner et al, 2009) should have the additional advantage of providing, in case of modern water, a “discrete age” for the sampled water, even though it needs complex and expensive measuring techniques and to this reason we will try to apply this method only as last check of our conceptual model.

### Geophysical investigations

In addition to geochemical methods we are interested in the use of geophysical approaches, in order to (i) predict the presence of fractures and discontinuities that are the preferable hydraulic pathways of the rock masses, (ii) forecast the possible water inflows in the tunnel, and (iii) investigate the hydrogeological behaviour of the water springs in the regions surrounding the new tunnel actually in construction. In our research project, we use a Very Low Frequency electromagnetic (VLF-EM) instrument and an Inductive Polarized (IP) Electrical Resistivity Tomography (ERT) equipment. Our aim is to better understand the possible application of the two approaches to investigate the interaction of tunnel with groundwater in the rock masses domain, discuss benefits and disadvantages and make a comparison of these methods.

The VLF-EM method is useful for the detection of elongated, steeply dipping high-conductivity bodies, that can be due not only to water trapped in rock fractures and cavities, but also due to conductive bodies in the underground. The instrument utilizes the magnetic component of the electromagnetic field generated by long-distance

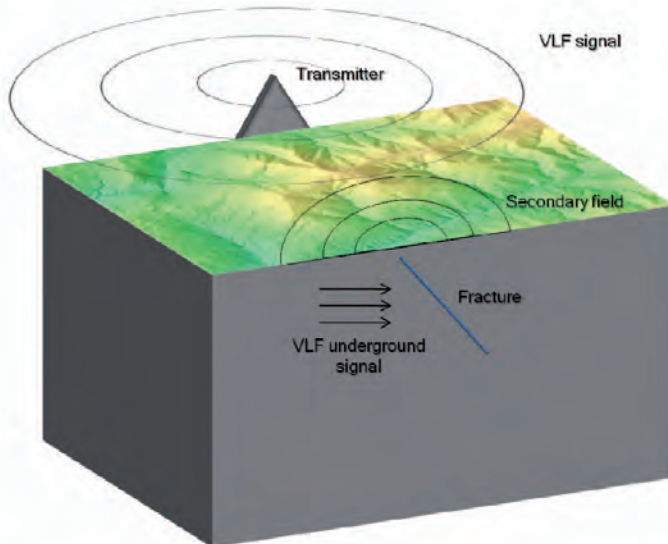


Fig. 12: Scheme of the VLF technique functioning

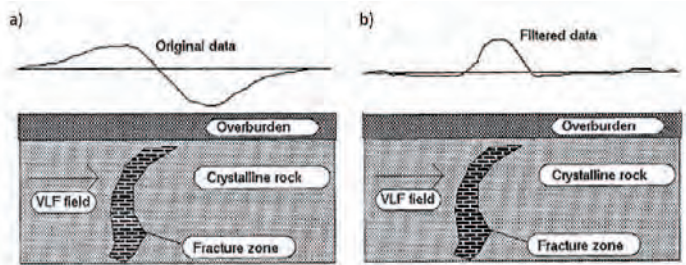


Fig. 13: Typical behaviour of an VLF anomaly like reached by the instrument (a) and after a filtering process of data (b)

radio transmitters in the very low frequency band (15-30 kHz), that are used mostly for long-distance communications. Conductive structures on the surface, but also in the underground, even when buried with a thick overburden, affect locally the direction and strength of the magnetic field normally generated by the transmitted radio signal. A weak secondary field builds up around the geological underground structure, and the instrument is capable to measure this radio signal distortion (Fig.12).

Therefore, VLF method has been often used in hydrogeology for the detection of fractures in rocks (Macedo and Lima, 2004). Few works have been carried out some years ago at Institute of Earth Sciences (IST-SUPSI) to find faults and fractures over tunnel (Pagano, 1996), in order to study hydrothermal flow of groundwater, or simply to test the instrument (Ghirlanda, 1996). Actually we want to test this method and to compare it with other geophysical methods. For this purpose, we use a WABEM® WADI VLF instrument of Institute of Earth Science (IST-SUPSI) of Lugano. The maximum depth capacity of the instrument is about 100 m, under ideal undisturbed conditions, and in particular it depends on the mean resistivity of the field rock. For a steeply dipping conductor, the typical anomaly will appear in the following manner: a maximum occurs to the left, and a minimum to the right of the conductor (Fig.13a). The above sketched anomaly can be imagined to be the real part, that is the part of the resulting field which are in phase with the primary field from the VLF transmitter. The instrument will also measure an imaginary component, which are 90° out of phase with the primary field. This way of plotting the VLF anomaly reached by the instrument, makes the interpretation of data difficult, especially in case of complicated geology. Various types of filtering techniques have been used to extract interesting information; in particular the WADI VLF instrument uses a filter designed by Karous an Hjelt (Abem, 1993) to purify the data. The output from this filter is an equivalent current density at a certain depth in the ground, that is named “anomaly” and is represented by a single peak right above the conductor (Fig. 13b). For the interpretation of recorded VLF data, we could use the RAMAG 2.2 software. It allows to download data from the instrument and to transform field data into line graphs of original and filtered data, and more understandable cross sections with % of in-phase response of underground to electrical current flow.

We are also performing some 2D geoelectrical surveys in order to test their application for the detection of fractures that could intersect the underground infrastructure, causing consistent water inflows within the tunnel actually excavating. The purpose of Electrical Resistivity Tomography (ERT) is to determine the subsurface resistivity distribution, by making more simple measurements on the ground surface (Fig.14). The resistivity  $\rho$  is the physical property which determines the aptitude of a material to oppose to the passage of the electrical current. In field geology, it is related to various ground parameters, such as the mineral and fluid content. In particular, knowing

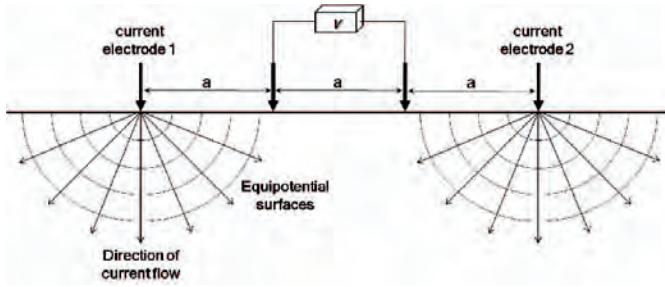


Fig. 14: Simplify pattern of resistivity acquisition. Two electrodes are used as electrical input, while two electrodes measure the difference of potential.

the geology and the resistance expected from a rock, often, the conductivity skill is mainly controlled by voids presence and by the water which they contain. For this reason, geoelectrical techniques are frequently used in the hydrogeological domain (Giudici et al., 2003).

A 2D acquisition uses a great number of electrodes connected to a multicore cable and placed along the desired profile. In the field we obtain values of terrain *apparent resistivity*, that is the resistivity of a homogeneous underground that will give the same resistance value for the same electrode arrangement. After both a filtering and an inversion process, the result is a modeled profile of terrain resistivity. In particular, using different configurations (Fig. 15), it is possible to analyze the superimposed horizontal layers of a terrain or the presence of vertical structures, such as faults or fractures in the rock components.

In the Ceneri Zone, due to the high elevation of the terrain above the tunnel, it is impossible to directly find the intersection between the eventually detected disturbed zones and the tunnel in construction; nevertheless geoelectrical surveys, connected with geomorphologic observations, can be useful in order to obtain information about location and properties of fractures or faults, even only in the shallow decompressed zone. To test it, we are using a 10 channel resistivity meter for resistivity and IP measurements (*Syscal Pro*) kindly provided by the Institute of Geophysics of University of Lausanne. For the download and the inversion of field data we are using the RES2DINV inversion software (Locke, 2004).

**Preliminary results of geochemical analysis**

For the region surrounding the new infrastructure of the Ceneri base tunnel there are about 750 springs registered in the cantonal hydrogeological database. On the basis of criteria of relevance (use and discharge), distance from the tunnel and chemico-physical preliminary characterization, a number of springs have been classified at high risk and selected for monthly measurements in the tunnel geological design (Colombi & Baumer, 1995). We have used this official

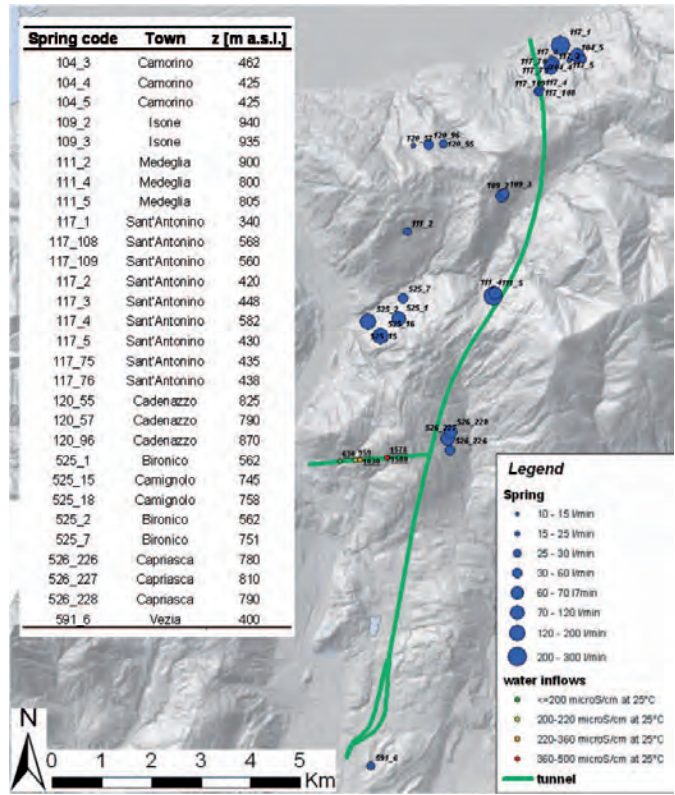


Fig. 16: Spring and water inflows monitored.

classification, in order to implement our monitoring network for isotopes measurements (Fig.16); in total, we are monitoring 29 springs. Monthly sampling of water of the selected springs for isotopic abundance data, we have performed also, if possible, physical measurements (discharge, conductivity, pH, air and water temperature). The monitoring will be performed for one year.

The spring waters come from different aquifers, most of which are silicate rocks (ortho-and paragneisses, micaschists, amphibolites, etc). Average annual discharges of monitored springs (1994-2009) vary from 15 to 300 l/min, electric conductivities from 50 to 300  $\mu\text{S/cm}$  at 25°C. These are typical values of water with low and very low ion concentrations with pH-values from 6 to 7.5, that are typical values of neutral waters. Discharge vary from season to season and recently increased, in consideration of that the last years (2008-2009) were very humid if compared with the standard Swiss precipitation rates (calculated on the 30 years between 1961 and 1990).

A number of chemical measurements (table 2) for a few of the se-

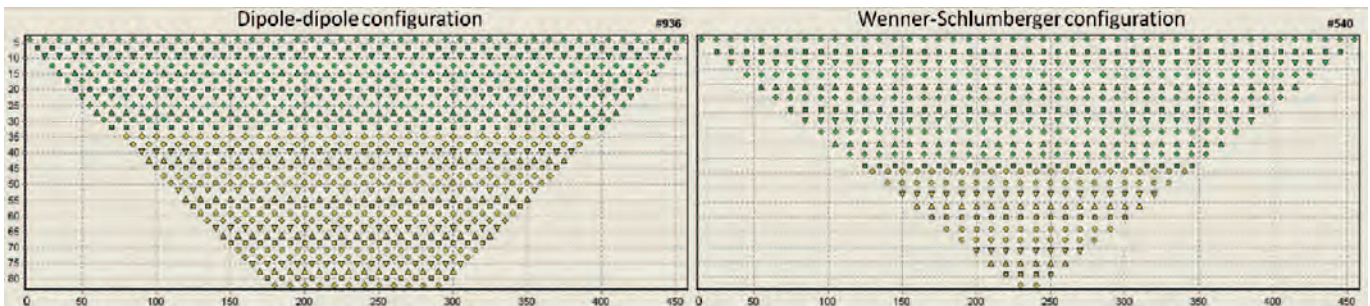


Fig. 15: Two possible configurations used to acquire the apparent resistivity values along a profile using 48 electrodes interspaced 10 m

**Tab. 2:** Results of chemico-physical analysis on springs (from Colombi et al., 1995)

| Spring ID   | 104_3                                | 117_1  | 117_3                 | 117_5                                      | 117_75             | 525_18              | 525_2                                | 525_7                                | 526_227                              | 526_228                              | 591_6                      |
|---|--------------------------------------|--|-----------------------|--|--------------------|---------------------|--------------------------------------|--------------------------------------|--------------------------------------|--------------------------------------|----------------------------|
| Flow (l/min)  | 8.4                                  | 62.7   | 21                    | 6  | 11                 | 51                  | 150                                  | 40                                   | 80                                   | 190                                  | 33                         |
| T(°C)   | 8.5                                  | 11.6   | 10.2                  | 11.3                                       | 8.2                | 7                   | 7.5                                  | 9.1                                  | 10                                   | 9.5                                  | 11.4                       |
| pH  | 6.6                                  | 6.2  | 6.3                   | 6.4  | 6.7                | 7.3                 | 7.1                                  | 7.1                                  | 6.8                                  | 6.6                                  | 6.3                        |
| Cond<br>( $\mu\text{S}/\text{cm } 20^\circ\text{C}$ ) | 66                                   | 105  | 62                    | 76   | 63                 | 113                 | 140                                  | 66                                   | 81                                   | 77                                   | 55                         |
| O (%)   |                                      |  | 92                    | 78   |                    |                     |                                      | 91                                   |                                      |                                      |                            |
| Ca (mg/l)   | 7.2                                  | 10.1   | 6.7                   | 7.8  | 6.7                | 20.8                | 26                                   | 10                                   | 10.5                                 | 10.4                                 | 6                          |
| Mg (mg/l)   | 1.3                                  | 2  | 1.1                   | 1.9  | 0.8                | 0.8                 | 2.4                                  | 0.9                                  | 1.5                                  | 1.1                                  | 0.9                        |
| Na (mg/l)   | 2.2                                  | 4.9  | 3.2                   | 4  | 2.4                | 1.2                 | 2                                    | 2.4                                  | 2.7                                  | 3.3                                  | 2.1                        |
| K (mg/l)  | 1.8                                  | 2.9  | 3.2                   | 0.8  | 1.4                | 1.4                 | 2.1                                  | 1.3                                  | 1.7                                  | 1.5                                  | < 1                        |
| NH <sub>4</sub> (mg/l)                                | 0.03                                 | 0.02   | 0.03                  | 0.04                                       | 0.02               | 0.02                | 0.02                                 | 0.02                                 | 0.03                                 | < .015                               | 0.03                       |
| HCO <sub>3</sub> (mg/l)                               | 9                                    | 16.1   | 6.7                   | 10.9                                       | 6.3                | 42.6                | 51.4                                 | 25.9                                 | 22.5                                 | 20                                   | 11.2                       |
| SO <sub>4</sub> (mg/l)                                | 14.4                                 | 14.1   | 15.3                  | 20.2                                       | 12.2               | 4.4                 | 17.7                                 | 7.7                                  | 13.4                                 | 19.4                                 | 2.2                        |
| NO <sub>3</sub> (mg/l)                                | < 1                                  | 8.4  | 2.1                   | < 1  | 3.1                | 3.5                 | < 1                                  | 1.5                                  | 2                                    | 1.4                                  | 1.6                        |
| Cl (mg/l)   | 1.6                                  | 4.2  | 1.5                   | 1.1  | 1.9                | 1.9                 | 2.4                                  | 1.6                                  | 1.4                                  | 1.4                                  | 3.6                        |
| NO <sub>2</sub> (mg/l)                                |                                      | < .05  | < .05                 | < .05                                      |                    |                     |                                      | < .05                                | < .05                                | < .05                                |                            |
| F (mg/l)  |                                      | < .1   | < .1                  | < .1                                       |                    |                     |                                      | < .1                                 | < .1                                 | < .1                                 |                            |
| SiO <sub>2</sub> (mg/l)                               |                                      | 12.7   | 12.9                  | 15.2                                       |                    |                     |                                      | 12.4                                 | 10.6                                 | 10.5                                 |                            |
| TDS (mg/l)  | 38.5                                 | 75.6   | 52.9                  | 63.1                                       | 34.8               | 76.6                | 105.0                                | 63.9                                 | 66.5                                 | 69.2                                 | 28.6                       |
| Water Type<br>(PHREEQC software)                      | Ca-SO <sub>4</sub> -HCO <sub>3</sub> | Ca-Na-SO <sub>4</sub> -NO <sub>3</sub> -HCO <sub>3</sub> | Ca-Na-SO <sub>4</sub> | Ca-Na-Mg-SO <sub>4</sub> -HCO <sub>3</sub> | Ca-SO <sub>4</sub> | Ca-HCO <sub>3</sub> | Ca-HCO <sub>3</sub> -SO <sub>4</sub> | Ca-HCO <sub>3</sub> -SO <sub>4</sub> | Ca-HCO <sub>3</sub> -SO <sub>4</sub> | Ca-SO <sub>4</sub> -HCO <sub>3</sub> | Ca-Na-HCO <sub>3</sub> -Cl |

lected springs in the region surrounding the Monte Ceneri base tunnel are available on the basis of geological structure of the tunnel (Colombi & Baumer, 1995). Other chemical measurements were carried out in November 2009 for all the selected springs (table 3). In addition to the general parameters (EC, T, discharge and pH) that were monthly monitored, we performed also geochemical analyses of major ions, total nitrogen, organic and inorganic carbon.

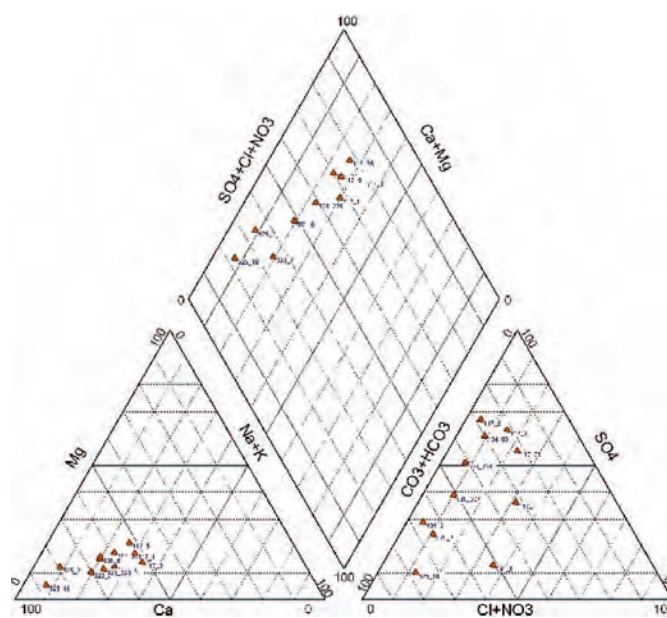
These analyses were carried out in the classical geochemistry laboratory of University of Lausanne (IMG-Centre d'Analyse Minerale). In particular F<sup>-</sup>, Cl<sup>-</sup>, NO<sub>2</sub><sup>-</sup>, NO<sub>3</sub><sup>2-</sup>, SO<sub>4</sub><sup>-</sup>, Li<sup>+</sup>, Na<sup>+</sup>, NH<sub>4</sub><sup>+</sup>, K<sup>+</sup>, Mg<sup>+</sup>, Ca<sup>+</sup> have been determined by Ion Chromatography, while HCO<sub>3</sub><sup>-</sup> is determined by mass balance with the total inorganic carbon, that is analyzed by a C-analyzer (LiquiTOC Elementar), together with organic carbon and total nitrogen.

From the position on the Piper diagram, we note that most of the springs are Ca-SO<sub>4</sub> or Ca-HCO<sub>3</sub>-type waters (Fig. 17 e 18), which are typically shallow groundwaters that flow through crystalline sulfide-bearing rocks; moreover this indication is confirmed by the low EC values. In particular it is possible distinguish between the Camorino and Sant'Antonino springs located above the northern portal, and the other waters, as well shown by figure 18.

We are also collecting a number of samples of the water inflows in the accessible tunnel (Sigirino exploration tunnel) and in the part of the tunnel actually in construction. Concerning the Sigirino access tunnel, we have a few of samples that were collected in the excavation phases by Altransit geologists; that kindly allow us, from now on, every two months, where possible, to sample the few residual water inflows. For the remaining parts of the tunnel, that are now drilled, we can collect also, samples of water inflows compatible with excavations works. This concerns in particular the few months of excavation at the northern portal, while the drilling at the southern portal will

start in april 2010.

What the isotopes concern, as first stage, using the least squares fit linear correlation method on 204 (49 of these were monthly sporadically collected by IAEA in the years since 1983 to 1991, 155 were monthly regularly collected by NISOT, that kindly offers our these data, in the years since 1992 to 2006) samples of water collected in Locarno Monti meteorological station, we have found a best fit line,

**Fig. 17:** Piper diagram of spring analyzed (elaborated from Colombi et al., 1995)

**Tab. 3:** Results of chemico-physical analysis on springs (november 2009)

| Spring  | Date (2009) | pH   | T (°C) | Cond (µS/cm 25 °C) | Q (l/min) | Na (mg/l) | K (mg/l) | Mg (mg/l) | Ca (mg/l) | F (mg/l) | Cl (mg/l) | NO <sub>3</sub> (mg/l) | SO <sub>4</sub> (mg/l) | HCO <sub>3</sub> (mg/l) | TDS (mg/l) | Water Type (PhREEQC software)                         |
|---------|-------------|------|--------|--------------------|-----------|-----------|----------|-----------|-----------|----------|-----------|------------------------|------------------------|-------------------------|------------|---|
| 104_3   | 13/11       | 6.70 | 10.1   | 80                 | 12        | 3.08      | 0.86     | 2.11      | 7.10      | 0.12     | 0.65      | 2.60                   | 22.45                  | 1.94                    | 40.94      | Ca-Mg-Na-SO <sub>4</sub>                              |
| 104_4   | 13/11       | 6.60 | 12.1   | 98                 | 105       | 3.72      | 1.54     | 2.62      | 16.90     | 0.11     | 1.35      | 3.78                   | 26.40                  | 18.41                   | 74.86      | Ca-SO <sub>4</sub> -HCO <sub>3</sub>                  |
| 104_5   | 13/11       | 6.60 | 9.9    | 80                 | 14        | 3.08      | 0.84     | 2.16      | 14.31     | 0.13     | 0.65      | 2.48                   | 23.08                  | 39.47                   | 86.23      | Ca-HCO <sub>3</sub> -SO <sub>4</sub>                  |
| 109_2   | 25/11       | 6.67 | 9.5    | 42                 | 17.6      | 2.54      | 1.05     | 1.38      | 12.40     | 0.05     | 1.16      | 4.60                   | 7.13                   | 40.50                   | 70.83      | Ca-HCO <sub>3</sub>                                   |
| 109_3   | 25/11       | 6.75 | 9.5    | 75                 | n.d.      | 3.17      | 1.14     | 2.50      | 17.85     | 0.06     | 1.34      | 5.04                   | 6.78                   | 66.97                   | 104.88     | Ca-HCO <sub>3</sub>                                   |
| 111_2   | 25/11       | 6.60 | 11.1   | 69                 | 12.5      | 2.47      | 1.22     | 1.26      | 7.51      | 0.06     | 0.68      | 3.27                   | 5.54                   | 28.98                   | 51.02      | Ca-HCO <sub>3</sub>                                   |
| 111_4   | 25/11       | 7.60 | 8.7    | 96                 | n.d.      | 1.58      | 0.48     | 2.34      | 12.55     | 0.05     | 0.67      | 5.68                   | 6.11                   | 49.27                   | 78.75      | Ca-HCO <sub>3</sub>                                   |
| 111_5   | 25/11       | 7.50 | 11     | 97                 | 30        | 1.63      | 0.82     | 4.25      | 14.05     | 0.16     | 0.75      | 5.71                   | 8.01                   | 53.09                   | 88.50      | Ca-Mg-HCO <sub>3</sub>                                |
| 117_1   | 13/11       | 6.50 | 11.6   | 118                | 150       | 5.79      | 2.48     | 2.69      | 9.76      | 0.13     | 7.27      | 7.04                   | 20.40                  | 25.71                   | 81.30      | Ca-Na-Mg-SO <sub>4</sub> -NO <sub>3</sub> -Cl         |
| 117_2   | 13/11       | 6.50 | 11.6   | 118                | 150       | 3.53      | 1.60     | 2.38      | 13.28     | 0.12     | 1.98      | 5.53                   | 20.02                  | 15.27                   | 63.74      | Ca-SO <sub>4</sub> -HCO <sub>3</sub>                  |
| 117_108 | 13/11       | 6.60 | 9.8    | 72                 | 32        | 3.82      | 0.92     | 2.00      | 7.11      | 0.10     | 2.34      | 5.63                   | 13.47                  | 31.51                   | 66.94      | Ca-HCO <sub>3</sub> -SO <sub>4</sub> -NO <sub>3</sub> |
| 117_109 | 13/11       | 6.60 | 9.9    | 73                 | 10        | 3.87      | 0.93     | 2.11      | 15.97     | 0.12     | 2.34      | 5.20                   | 13.72                  | 62.29                   | 106.59     | Ca-HCO <sub>3</sub> -SO <sub>4</sub>                  |
| 117_5   | 13/11       | 6.80 | 10.6   | 90                 | 12        | 3.94      | 0.87     | 2.66      | 8.07      | 0.15     | 0.79      | 0.65                   | 24.66                  | 21.55                   | 63.37      | Ca-Mg-SO <sub>4</sub> -HCO <sub>3</sub>               |
| 117_75  | 13/11       | 6.80 | 10.7   | 78                 | 8         | 4.07      | 0.81     | 1.82      | 11.16     | 0.11     | 4.25      | 3.56                   | 16.08                  | 11.49                   | 53.39      | Ca-Na-SO <sub>4</sub> -HCO <sub>3</sub>               |
| 117_76  | 13/11       | 6.40 | 10.4   | 80                 | 15        | 4.08      | 0.91     | 1.91      | 16.28     | 0.11     | 4.13      | 3.71                   | 15.90                  | 30.87                   | 77.93      | Ca-HCO <sub>3</sub> -SO <sub>4</sub>                  |
| 120_55  | 16/11       | 6.98 | 8.5    | 56                 | 38.8      | 2.32      | 0.89     | 1.06      | 11.69     | 0.07     | 0.51      | 9.56                   | 9.89                   | 36.46                   | 72.47      | Ca-HCO <sub>3</sub> -NO <sub>3</sub> -SO <sub>4</sub> |
| 120_57  | 16/11       | 6.36 | 8.8    | 50                 | 23.1      | 2.08      | 0.75     | 1.02      | 8.50      | 0.06     | 0.55      | 6.20                   | 4.24                   | 24.84                   | 48.26      | Ca-HCO <sub>3</sub> -NO <sub>3</sub>                  |
| 120_96  | 16/11       | 6.89 | 8.2    | 70                 | 40.1      | 2.23      | 0.71     | 1.01      | 12.21     | 0.06     | 0.41      | 6.21                   | 6.12                   | 35.98                   | 64.97      | Ca-HCO <sub>3</sub> -NO <sub>3</sub>                  |
| 525_1   | 25/11       | 7.30 | 8.4    | 73                 | 50        | 2.31      | 1.02     | 1.47      | 10.36     | 0.13     | 0.67      | 3.38                   | 5.78                   | 49.91                   | 75.05      | Ca-HCO <sub>3</sub>                                   |
| 525_15  | 25/11       | 7.70 | 8.3    | 130                | 80        | 2.28      | 0.66     | 1.52      | 21.35     | 0.27     | 0.61      | 5.04                   | 11.93                  | 47.27                   | 90.96      | Ca-HCO <sub>3</sub>                                   |
| 525_18  | 25/11       | 7.60 | 7.6    | 120                | 2.8       | 2.17      | 0.88     | 1.42      | 19.86     | 0.28     | 0.57      | 5.39                   | 11.58                  | 57.12                   | 99.28      | Ca-HCO <sub>3</sub>                                   |
| 525_2   | 25/11       | 7.40 | 9      | 157                | n.d.      | 2.94      | 1.98     | 2.86      | 24.52     | 0.19     | 0.84      | 1.59                   | 24.85                  | 55.51                   | 115.31     | Ca-HCO <sub>3</sub> -SO <sub>4</sub>                  |
| 525_7   | 25/11       | 7.40 | 8.7    | 133                | n.d.      | 3.05      | 1.90     | 2.84      | 19.93     | 0.12     | 0.84      | 2.75                   | 12.04                  | 59.76                   | 103.26     | Ca-HCO <sub>3</sub>                                   |
| 526_226 | 19/11       | 6.80 | 10.1   | 95                 | 85.3      | 3.35      | 1.39     | 2.11      | 10.05     | 0.08     | 0.86      | 2.85                   | 18.97                  | 33.23                   | 72.91      | Ca-HCO <sub>3</sub> -SO <sub>4</sub>                  |
| 526_227 | 19/11       | 6.80 | 9.8    | 99                 | 60        | 2.91      | 1.47     | 2.05      | 10.56     | 0.07     | 1.09      | 4.03                   | 16.73                  | 32.64                   | 71.57      | Ca-HCO <sub>3</sub> -SO <sub>4</sub>                  |
| 526_228 | 19/11       | 6.75 | 9.7    | 93                 | 85.7      | 3.02      | 1.58     | 2.18      | 20.80     | 0.07     | 0.85      | 2.83                   | 20.26                  | 44.59                   | 96.21      | Ca-HCO <sub>3</sub> -SO <sub>4</sub>                  |
| 591_6   | 25/11       |      | 11.7   | 85                 | 23.1      | 3.82      | 0.81     | 2.35      | 14.81     | 0.25     | 2.10      | 3.54                   | 9.23                   | 47.28                   | 84.95      | Ca-HCO <sub>3</sub>                                   |

**Tab. 4:** Different correlation lines for stable isotopic composition of springs and tunnel inflows. There is no clear distinction between various waters.

| Water type                         | Correlation lines                            | Correlation coefficient |
|------------------------------------|--|-------------------------|
| Tunnel inflows                     | $\delta^2H = 6.73 \cdot \delta^{18}O + 3.81$ | $r^2=0.92$              |
| Camorino and Sant'Antonino springs | $\delta^2H = 6.68 \cdot \delta^{18}O + 3.19$ | $r^2=0.95$              |
| Veduggio groundwater basin springs | $\delta^2H = 6.71 \cdot \delta^{18}O + 3.81$ | $r^2=0.97$              |

which we can be defined as “Locarno meteoric line” (Fig. 19).

It is expressed by the following linear correlation:

$$\delta^2H = 7.79 \delta^{18}O + 5.65 \quad (9)$$

With a correlation coefficient  $r^2$  value of 0.96.

Actually, we have only analyzed stable isotopes in a few of the water collected on the surface springs and within the tunnel. Deuterium and oxygen-18 analyses were performed at the Stable Isotopes Laboratory of the University of Lausanne, using a Wavelength-Scanned Cavity Ring Down Spectroscopy (WS-CRDS) based analyzer that perform together deuterium and oxygen-18 analysis. For seasonal feedbacks and mean altitude recharge evaluation it is necessary to complete the scheduled year of observation; nevertheless a preliminary comparison with meteorological water lines, and a dis-

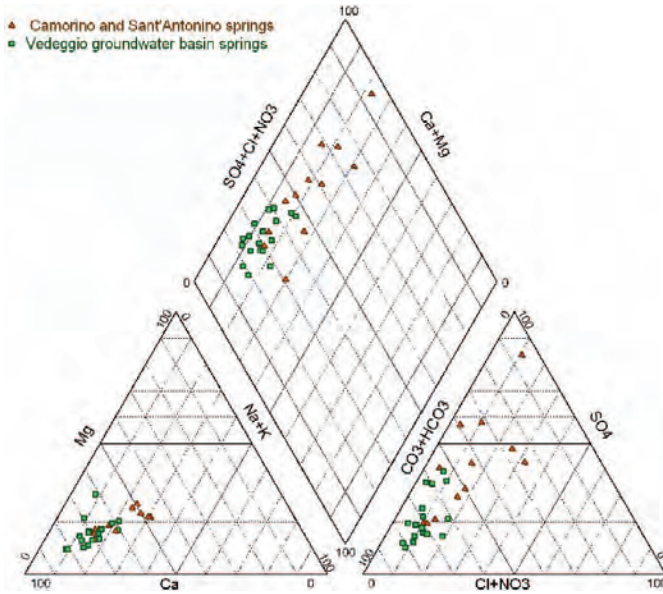


Fig. 18: Piper diagram of spring analyzed monitored (data of November 2009)

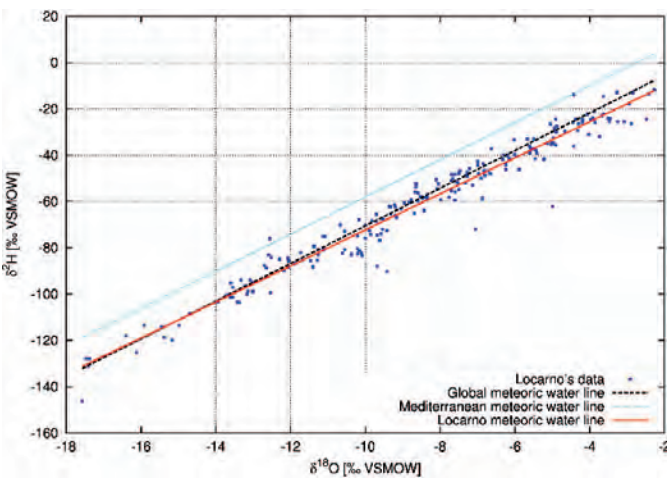


Fig. 19: Stable isotopes composition in Locarno precipitations. Local data are fitted by equation 9 and compared with the Vienna Meteoric Water Line (Rozanski et al., 1993)

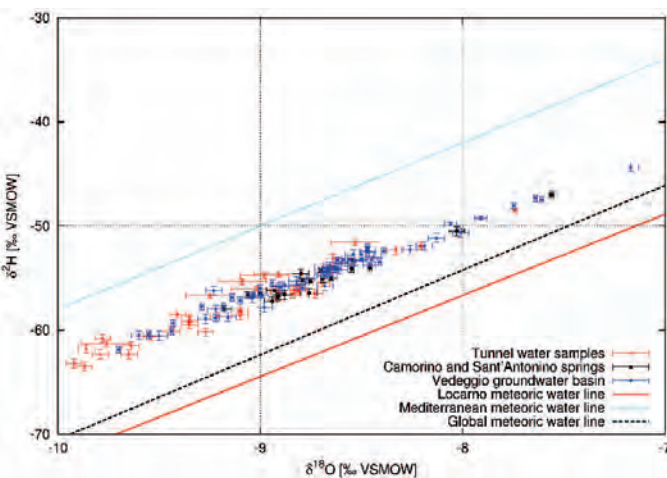


Fig. 20: Stable isotopic composition of spring's water and Sigirino tunnel inflows.

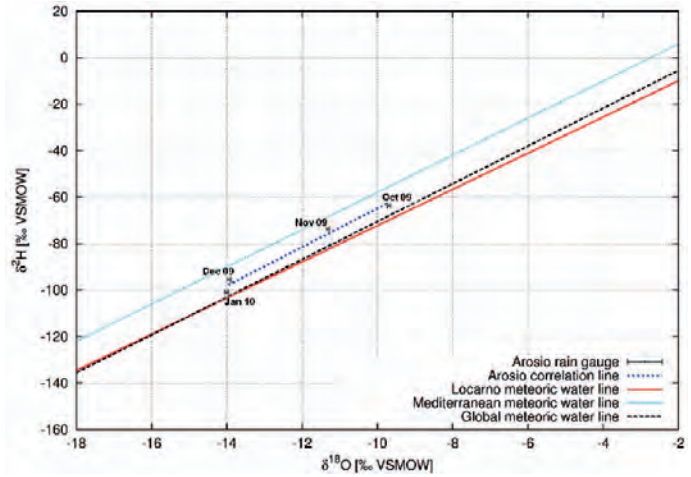


Fig. 21: Stable isotopes composition in Arosio precipitations compared with existent meteoric water lines.

tion between isotopic composition of spring water and that of the inflows in the Sigirino prospection tunnel is possible using a  $\delta^2H$  and  $\delta^{18}O$  graphic correlation (fig.20). In particular Sigirino tunnel data (red star) are almost all displaced between the Mediterranean and the global or local (Locarno) meteoric water lines. Nevertheless considering the interpolation process which are used in order to obtain the Locarno meteoric line, and the altitude effect on the Monte Ceneri area, these are, reasonably, the typical meteoric water of our region, with relative small residence time. We also try to distinguish between the Camorino and Sant'Antonino springs (black square) located above the northern portal, and the other groundwaters of the Vedeggio hydrogeological basin (blue circle), but there is no clear difference, as shown also by three different correlation lines reported in table 4. All the data analyzed up to now are collected between June and November 2009, and are characterized by relative high values in  $\delta^2H$  and  $\delta^{18}O$  compared to winter precipitation values, that are well shown by figure 21.

Also the few precipitation samples, collected in the Arosio rain gauge are analyzed and the obtained stable isotope abundance values are also reported on the  $\delta^2H$  and  $\delta^{18}O$  diagram (fig.21). A first correlation between data is possible:

$$\delta^2H = 8.32 \delta^{18}O + 18.35 \tag{10}$$

Where correlation coefficient value  $r^2$  is 0.97.

Obviously the quality is not good, because of the lack of the necessary number of samples (at least one year of observation).

### Preliminary results of geophysical surveys

Initially, in spring and summer 2009, we have carried out some tests about the applications of two geophysical methods above mentioned. Obtaining good results, we have performed an out-and-out geophysical survey in October 2009 in the Monte Ceneri base tunnel area, specifically designed for the detection of the possible discontinuities of the rock masses that are the preferential hydraulic pathways in this geological medium. The eight realized profiles are shown in figure 22. For each profile, we have done both the VLF electromagnetic profile and the 2D geoelectrical tomography. In particular, where possible, we have investigated with our surveys both the Val Colla line and the region close to the Isonne town where the most important disturbed zones are expected. In the next months we will realize also two other geophysical campaigns designed for the water inflows prediction and

hydrogeological characterization of water springs.

The detailed results of the carried out geophysical surveys will be presented in further specific publications. In this paper we restrict ourselves to few preliminary considerations about the hydrogeological use of these methods, putting the emphasis on their benefits and disadvantages. Geoelectrical surveys are more expensive with respect to VLF electromagnetic profiles. In fact, ERT method request three or four people for the displacement of electrical cables and instrument, while VLF surveys request only a single operator, because it is a lighter instrument. Nevertheless geoelectrical results, in our opinion, are more reliable. In fact a 2D resistivity model of the underground is given, inverting, with an iterative procedure, the apparent resistivity values that the instrument reads in field. For each resistivity profile, an index of the goodness of the data is given by the RMS error, that is the difference between the real apparent resistivity values recorded in field by the instrument and that calculated on the hypothetical model of underground resistivity. Therefore RMS errors lower than 10 are typical of a very good model, values between 10 and 20 are indicative of discrete model of resistivity, while RMS errors higher than 20 are typical for a bad terrain model.

Contrarily, the VLF results are less clear. In fact there is not always a direct correlation between the resulting profile and the geology. The instrument simply detects and maps electrical conductive zones. Data units are expressed in percentage of the in-phase response produced by the subsurface matrix; obviously the % of in-phase answer

is linked with the degree of conductivity of rock masses or soil, but there is no direct correlation between % in-phase response and resistivity of the underground as in the resistivity method. Finally, unlike the ERT method, VLF results do not have an index of the goodness of data; the user is the only subject that is able to check the quality of field data and look for signs of noise and interferences, directly showing the data downloaded by the instrument.

As mentioned above, resistivity surveys are, in our opinion, more reliable to perform hypotheses on the underground geology. In fact resistivity values of crystalline rock, (such as gneiss, paragneiss, orthogneiss and amphibolites) are in general higher than 1000 ohm-m; therefore the presence of fractures, or in general disturbed zones with water is clearly indicated on geoelectrical profiles by an high increase of conductivity. Obviously there are also some critical situations; for example the presence of a moraine deposit is not always predictable, because different types of sediments produce also a heterogeneity in resistivity values. In particular, sands and gravels should cause an increase in conductivity, while the presence of rock inside the deposit can increase the resistivity values. Also the occurrence of water, for example of a water table within the glacial deposit, is another factor that complicates the geophysical interpretations in this geological environment. On the contrary, in any cases a difference in electrical response is even observable, between two type of rocks, such as in the Bigorio 2 survey (Fig. 23) that we show here as example of the obtained geophysical results. In this case, we have measured the profile intersecting the previous cited Val Colla disturbed zone, where the geological map which shows a transition from Giumiello to Stabiello gneisses (Fig 23a). Results of ERT (Fig 23b), even more disturbed with respect to other profiles (RMS error is 13.9 %, while in the other profiles is always less than 10%), show very well the central presence of a zone characterized by high conductivity values, that is probably the Val Colla fault. Moreover a slight difference is visible at the right and left of this fault; Stabiello gneiss, in particular, seems to have an higher resistivity value compared with Giumiello gneiss.

VLF profiles are instead more disturbed. Data are expressed in % in-phase. As shown by figure 23c for the Bigorio 2 profile, some interfaces between different geological matrices seem perceptible, but there is not a clear correlation between geoelectrical and electromagnetic results, and these latter seem worse than ERT results.

## Considerations and perspectives

To study large scale flow systems in fractured crystalline rocks, a comprehensive study is actually ongoing in southern Switzerland (Canton Ticino), taking advantage of the availability of a large amount of geological and hydrogeological data collected in the region of Monte Ceneri, for the current construction of the railway base tunnel. A monitoring network of spring, rain and tunnel waters has been carried out for geochemical, physical, oxygen and hydrogen isotopic water composition data, and the monitoring is currently underway. Moreover, we have performed few geophysical surveys to understand the availability of VLF-EM and ERT methods to detect fractures and faults in the underground, that could be the hydraulic pathways of the rock masses.

Physical (discharge, conductivity, pH and temperature), and chemical measurements are nowadays the only available and reasonable methods, with which we can obtain indications about groundwater system before the drilling of a new infrastructure starts, and therefore to understand the possible interaction between the tunnel and the groundwater flows in the fractured rock matrix. The collection of data, with an appropriate monitoring network is always possible, not

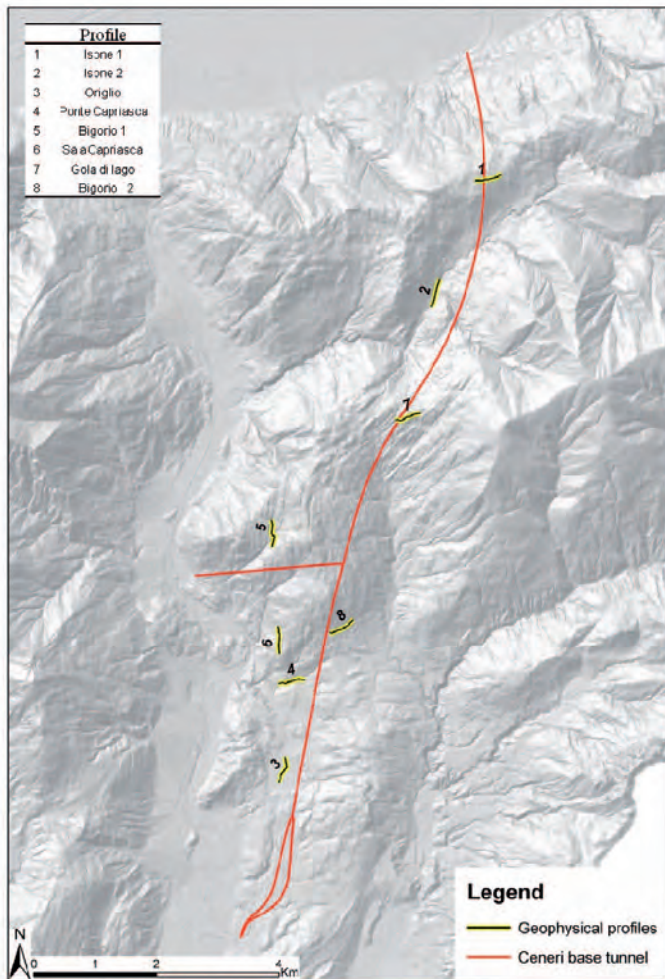
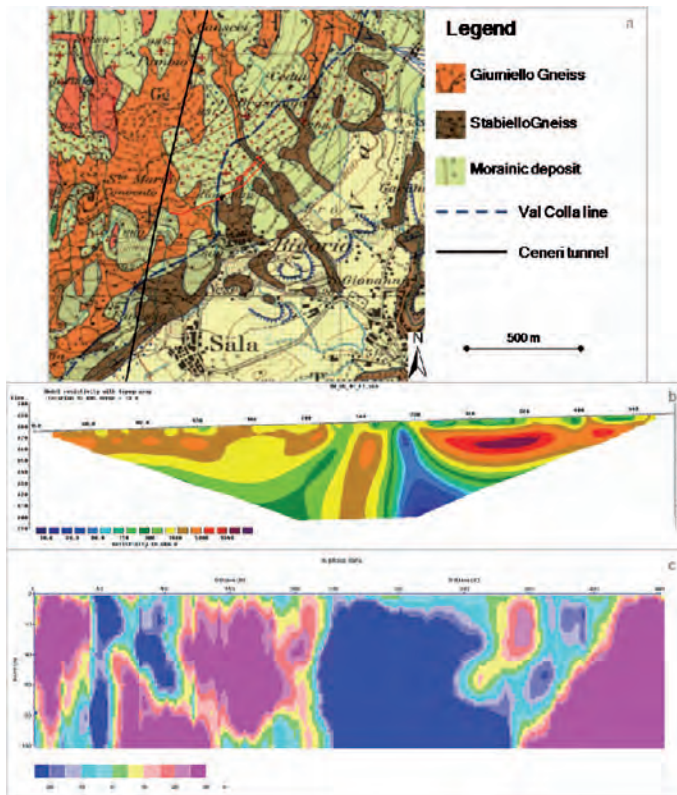


Fig. 22: Geophysical profiles location



**Fig. 23:** Profile 8: a) trace of geophysical profile on the geological map (1:25000); b) resistivity profile; c) VLF electromagnetic profile.

expensive and very functional.

Moreover we expect also useful information from the application of isotopic techniques. In fact, the monthly collection of stable isotopes of hydrogen and oxygen will give us indication on (i) water origin, (ii) type of recharge and (iii) residence time of water in the underground.

Actually the application of geophysical methods to detect discontinuities that constitute the preferential hydraulic pathways in the rock masses is not able to give us a physical validation of results obtained, because the tunnel will not be excavated exactly below the survey locations. Nevertheless, especially for the resistivity method, comparing them with geological existing map, geomorphological and surface geological observations, and deeper tunnel indications, we have obtained reliable results. VLF electromagnetic data are generally more disturbed and not always appear reliable, even if, considering the manageability of this technique, it could be applied as indication method, at least in a preliminary stage of a construction of a new tunnel. Besides, more detailed considerations and a specific comparison between the two methodology will be carried out near the north portal where the tunnel excavation will take place at a lower depth and using a new smaller case study where seismic methods have been already been applied, allowing a better physical validation of the geophysical hypothesis, that is otherwise impossible.

This paper present only the preliminary steps of a comprehensive study that we are carrying out in the Southern Switzerland, where few tunnels are actually excavating in metamorphic rocks. In particular, we have shown the configuring of the stable isotope monitoring network, the preliminary geochemical outcomes, and just an example of the results coming from the VLF-EM and the ERT methods; while in further publications the complete results of geochemical and isotope analysis and of geophysical surveys will be detailed presented. Nevertheless,

summarizing we could make some preliminary considerations.

Firstly, the low mineralization of spring waters like as the first geochemical analysis denote that all the springs are originated by shallow groundwater systems with a relative small residence time. The underground flows seem localized in the upper part of the rock masses that is characterized by an higher fracturation, confirmed also by the results of the first campaign of geoelectrical and electromagnetic surveys. Moreover, on the basis of the preliminary geochemical outcomes from collected samples, it is possible distinguish between two slightly different hydrochemical facies; one is typical of the springs located above the Vigana northern portal, and one of the other springs belonging to Vedeggio groundwater basin.

A second observation is that the rock mass fracturation and thence the hydraulic permeability decrease with the depth as shown by drilling inspections. This evidence is also confirmed by the excavation of the Sigirino access tunnel. In fact this part of tunnel has been excavated in dry conditions and moreover they are big differences between the hydrogeological facies of the spring waters and that of the inflows in the Sigirino access tunnel, that, although not presented in this paper, are typical of deeper aquifers.

Finally, due to these remarks, we could conclude that the possible interferences between the tunnel actually in construction and the most important water springs seem weak. Instead we could expect an interference with the surface water discharge, at least close to the north portal of the tunnel and in the high Vedeggio hydrological basin, where we expect few humid faults that could be a fast interconnection between the surface and the tunnel.

More detailed informations about the underground flows will be available after completing the stable isotope monitoring currently underway (until September 2010), from the tritium analysis, perhaps combined with helium, and thanks to the further applications of the geophysical surveys.

**Acknowledgements:** We will like to thank Alptransit San Gotardo Inc and in particular the Dr. Geol Pierre-François Erard and Geol. François Ghirlanda for the time expend for us, the helpfulness demonstrate and the data provided; the Dr. Eng. Ludovic Baron and Prof. Klaus Holliger of Institute of Geophysics (Unil) that kindly give us the geoelectrical instruments and the theoretical supports; and the Dr. Laurent Decrouy and Prof. Torsten Vennemann of the Stable Isotopes Laboratory (Unil) for the availability of the measurement instruments.

## References

- Abem (1993), Abem Wadi® VLF Instruction manual.
- Aeschbach-Hertig W, Schlosser P, Stute M, Simpson HJ, Ludin A, Clark JF (1998) A  $^3\text{H}/^3\text{He}$  study of ground water flow in a fractured bedrock aquifer, *Ground Water* 36(4):661-670
- Althaus R, Klump S., Onnis A., Kipfer R., Purtschert R., Stauffer F., Kinzelbach W. (2009), Noble gas tracers for characterisation of flow dynamics and origin of groundwater: A case study in Switzerland, *Journal of Hydrology* 370 (2009) 64-72
- Beatrizzotti G. (1996), *Cantone Ticino - Valutazione della permeabilità delle rocce*. 17pp
- Bestenheider J.C., (2006), *Captazioni nella Galleria OFIBLE, a 300 m e a 1210 m dal portale della finestra di Torre, Hydrogeological study for the Torre Town (Ticino-CH)*

- Colombi A, Baumer A (1995), Galleria di base del Monte Ceneri, Situazione idrogeologica, Rapporto idrogeologico, Technical report of the "Studio di geologia Dr. A. Baumer"
- Craig H., (1961), Isotopic variations in meteoric waters, *Science*, 133, 1702-1703
- Eichinger L, Merkel B, Nemeth G, Salvamoser J, Stichler W (1984), Seepage Velocity Determinations in Unsaturated Quarternary Gravel. Recent investigations in the Zone of Aeration, Munich 303–313.
- El Tani M (2003), Circular tunnel in a semi-infinite aquifer, *Tunnelling and Underground Space Technology*, 18(1):49-55
- Ghirlanda F (1996), Test effettuato con il VLF WADI ABEM. Internal report of IST
- Giudici M, Manera M, Romano E (2003), The use of hydrological and geo-electrical data to fix the boundary conditions of a ground water flow model: a case study, *Hydrology and Earth System Sciences*, 7(3):297-303
- Holzner CP, Aeschbach-Hertig W, Simona M, Veronesi M, Imboden DM, Kipfer R (2009), Exceptional mixing events in meromictic Lake Lugano (Switzerland/Italy), studied using environmental tracers 54(4):1113–1124
- Loke M.H. (2004), Tutorial:2-D and 3-D electrical imaging surveys Copy-right (1966-2004)M.H.Loke 136pp.
- Longinelli A, Anglesio E, Flora O, Iacumin P, Selmo E (2006), Isotopic composition of precipitation in northern Italy: reverse effect of anomalous climatic events. *J. of Hydrology*329:471-476
- Lucas LL, Unterweger MP (2000), Comprehensive review and critical evaluation of the half-life of tritium. *J. Res. Natl. Inst. Stand. Technol.* 105:541-549
- Macedo L, Lima AS, (2004), Groundwater exploration by VLF techniques: a case study in granitic terrains of Northwestern Portugal. In: Proceedings of the "2004 Fractured Rock Conference", National Ground Water Association, USA
- Maloszewski P, Moser H, Stichler W, Bertleff B, hedin K, (1990), Modelling of groundwater pollution by river bank filtration using oxygen-18 data Groundwater monitoring and management IAHS Publ. no 173:153-161
- Maréchal J.C. & Etcheverry D., (2003), The use of  $^3\text{H}$  and  $^{18}\text{O}$  tracers to characterize water inflows in Alpine tunnels, *Applied Geochemistry* 18:339-351
- Novel J.P., Dray M., Ferhi A., Jusserand C., Nicoud G., Olive P., Puig J.M. & Zuppi G.M., (1999), Homogénéisation des signaux isotopiques,  $^{18}\text{O}$  et  $^3\text{H}$ , dans un système hydrologique de haute montagne: la Vallée d'aoste (Italie), *Revue des sciences de l'eau* 12(1):3-21
- Offerdinger US, (2001), Ground water flow systems in the Rotondo Granite, Central Alps (Switzerland), Phd thesis of Natural Science, Swiss federal institute of technology (ETH) - Zurich
- Pagano A, (1996), Indagine geofisica VLF (Very Low Frequency) preliminare allo scavo della galleria per Mergoscia, Cantone Ticino. Technical reports of IST
- Pastorelli S (1999), Low enthalpy geothermal resources of the western alps. Geochemical and isotopic considerations and tectonic constraints. Examples from the cantons of Ticino and Bern (Switzerland), Phd thesis, Faculty of Geoscience, University of Lausanne
- Pearson F.J., Balderer W., Loosli H.H., Lehmann B.E., Matter A., Peters T., Schmassmann H. & Gautschi A., (1991), Applied Isotope Hydrogeology - A case study in Northern Switzerland, NAGRA Technical Report 88-01
- Pini O., Erard p.f. & Del Col A. (2007), Percer la base du Ceneri. *Traces* 22:16-22
- Schlosser P, Stute M, Dorr H, Sonntag C, Munnich KO (1988), Tritium/ $^3\text{He}$  dating of shallow groundwater, *Earth and Planetary Science Letters*, 89:353-362
- Schlosser P, Stute M, Sonntag C, Munnich KO, (1989), Tritiogenic  $^3\text{He}$  in shallow groundwater, *Earth and Planetary Science Letters*, v. 94, pp. 245-256
- Schurch M., Kozel R.; Schotterer U., Tripet JP, (2003), Observation of isotopes in the water cycle: the Swiss National Network (NISOT), *Environmental geology* 45(1):1-11
- Sheppard S.M.F (1986), Characterization and isotopic variations in natural waters. In: J.W. Valley, H.P. Taylor, Jr. and J.R. O'Neil, Editors, *Stable Isotopes in High Temperature Geological Processes Reviews in Mineralogy*, Mineralogical Society of America 16:165–183